IOPscience iopscience.iop.org

Home Search Collections Journals About Contact us My IOPscience

Multiphase composite coatings: structure and properties

This content has been downloaded from IOPscience. Please scroll down to see the full text.

2015 IOP Conf. Ser.: Mater. Sci. Eng. 81 012090

(http://iopscience.iop.org/1757-899X/81/1/012090)

View the table of contents for this issue, or go to the journal homepage for more

Download details:

IP Address: 82.200.251.6
This content was downloaded on 12/06/2015 at 10:06

Please note that terms and conditions apply.

Репозиторий КарГУ

# Multiphase composite coatings: structure and properties

**V M Yurov[1], S A Guchenko[1], E S Platonova[1], A Sh Syzdykova[1], E N Lysenko[2]**

[1]Buketov Karaganda State University, Karaganda, Kazakhstan
[2]National Research Tomsk Polytechnic University, Tomsk, Russia

E-mail: lysenkoen@tpu.ru

**Abstract.** The paper discusses the results of the research into the formation of ion-plasma multiphase coatings. The types of the formed structures are found to be not so diverse, as those formed, for example, in alloy crystallization. The structures observed are basically of globular type and, more rarely, of unclosed dissipative and cellular structures. It is shown that the properties of the coating formed in deposition are largely determined by its surface energy or surface tension. Since the magnitude of the surface tension (surface energy) in most cases is an additive quantity, each of the elements of the coating composition contributes to the total surface energy. In case of simultaneous sputtering of multiphase cathodes, high entropy coatings with an ordered cellular structure and improved mechanical properties are formed.

## 1. Introduction

The microstructure of single-phase films can be described qualitatively well using models proposed by Movchan and Demchishin, and Thornton [1, 2]. However, if the film is doped with impurities, these models greatly change. The columnar microstructure typical mainly of single-phase films completely changes in films with an average and high impurity content. This fact is described by the model developed by Barna and Adamik [3].

To obtain nanocomposites with plasma deposition methods, the multicomponent flows are to be deposited on the substrate. In most cases, the coating of a complex elemental composition is synthesized through layering or simultaneous deposition of the flows on a substrate in reactive gas atmosphere from sources: ion [4], magnetron [5], vacuum arc [6], and their combinations thereof. [7]

The paper presents the experimental data on the structure of multi-phase coatings and their properties. The results obtained are discussed in terms of the role of the surface tension in formation of the coatings.

## 2. Experimental

In the research, the Zn-Al, Al-Fe, Zn-Cu-Al, Mn-Fe-Cu-Al and Cr-Mn-Si-Cu-Fe-Al composite cathodes prepared by induction melting were used to deposit coatings. The technique of simultaneous sputtering of different cathodes in argon and nitrogen atmosphere was used as well.

The thickness of the coatings and their elemental composition were measured using an electron microscope 200 Quanta 3D. The phase composition and structural parameters of the samples were studied by means of the diffractometer XRD-6000 with CuKα-radiation. The phase composition, size of the coherent scattering regions and internal elastic stresses ($\Delta d/d$) were analyzed using PCPDFWIN and PDF4+ databases and the POWDER CELL 2.4 software was used for a full-profile analysis. The

Репозиторий КарГУ

nanohardness of the coatings was determined with the nano-identification system by the Oliver-Pharr method with the Berkovich indenter under a load of 1 g and the time of exposure of 15 s.

### 3. Results and discussion

Figures 1 and 2 show the images of Zn-Al and Fe-Al two-phase coatings obtained with an atomic force microscope. In the first case, the structure is globular, and in the second one, the structure is unclosed dissipative. We suppose that this difference in the structure of the coatings is caused by the difference in the surface tension of the basis metals of these coatings.

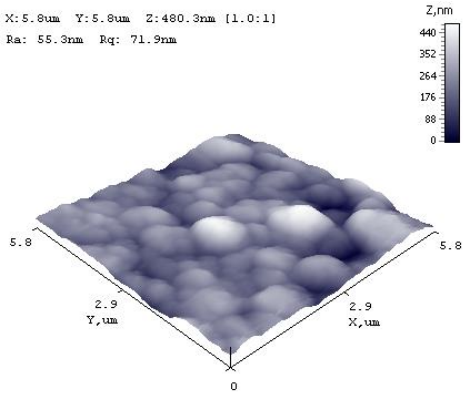


**Figure 1.** AFM image of the Zn-Al coating surface.

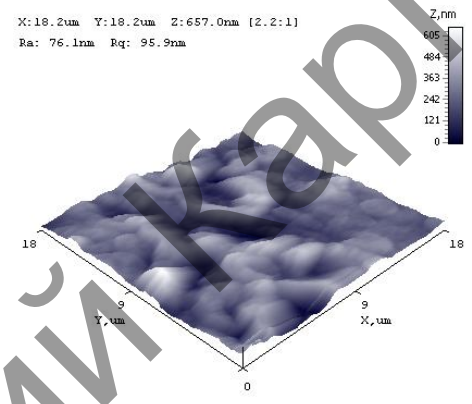


**Figure 2.** AFM image of the Fe-Al coating surface.

The surface tension for Zn-Al and Fe-Al coatings was determined by the technique described in [8]. The results obtained by the quantitative elemental analysis of the composite coatings were $Fe_{0.57}Al_{0.43}$ and $Zn_{0.34}Al_{0.66}$. The mean values of the surface tension were found to be $\sigma_{Fe\text{-}Al}$ = 0.972 J/m$^2$ and $\sigma_{Zn\text{-}Al}$=0. 617 J/m$^2$.

Using the values of the surface tension for pure metals [9], we obtain:

$$\sigma_{Fe\text{-}Al}= 0.57\cdot\sigma_{Fe}+0.43\cdot\sigma_{Al}=1.01 \text{ J/m}^2;$$

$$\sigma_{Zn\text{-}Al}= 0.35\cdot\sigma_{Zn}+0.65\cdot\sigma_{Al}=0.551 \text{ J/m}^2.$$

It can be seen that the experimental and theoretical values of the surface tension for Fe-Al and Zn-Al coatings coincide within the experimental error. The surface tensions for Fe-Al and Zn-Al coatings are two times different.

According to the classical theory, the nucleation of a new phase in from the metastable phase is regarded as a fluctuation process [10]. In this case, the work of the spherical nucleus formation is

$$W = \Delta F_{кр} = \frac{16\pi}{3}\left(\frac{M}{\rho}\right)^2 \frac{\sigma^3 T_0^2}{q^2(\Delta T)^2},$$

where $M$ is molecular weight, $\rho$ is nucleus density, $q$ is heat of fusion, $T_0$ is the equilibrium temperature of the two phases of infinite radius.

From the last expression it follows that the work of the globule formation is proportional to the cube of the surface tension. This indicates the importance of considering the surface tension of the components in plasma coating formation.

Figure 3 shows the structure of the coating prepared by simultaneous sputtering of Cr-Mn-Si-Cu-Fe- Al and titanium cathodes in nitrogen atmosphere.

Репозиторий КарГУ

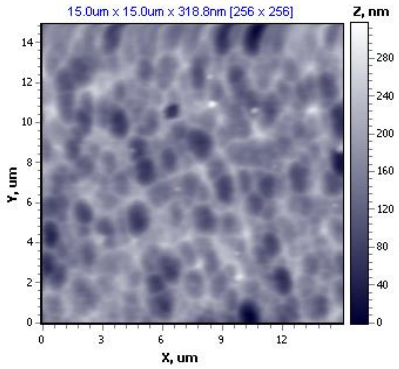


**Figure 3.** AFM images for the cellular structure of Cr-Mn-Si-Cu-Fe-Al + Ti coating in nitrogen atmosphere.

The results of the study of the phase composition and structural parameters of the sample are shown in Table 1. The nanohardness of Cr-Mn-Si-Cu-Fe-Al+Ti coating in nitrogen gas environment is 7.413 GPa. For 12X18H10T+Ti coating in nitrogen gas environment, the nanohardness is very high and is equal to 35.808 GPa. For comparison, Table 2 shows the nanohardness values for the most solid materials.

**Table 1.** Phase composition of Cr-Mn-Si-Cu-Fe-Al+Ti coating in nitrogen gas environment.

| Sample | Determined phases | Phase content, vol.% | Lattice parameters, Å | Coherent scattering region nm | $\Delta d/d^*$ $10^{-3}$ |
|---|---|---|---|---|---|
| Cr-Mn-Si-Cu- | $FeN_{0.0324}$ | 60.6 | a=3.598 | 103.37 | 3.460 |
| Fe-Al+Ti | $TiN_{0.31}O_{0.31}$ | 39.4 | a=4.211 | 25.6 | 5.143 |

**Table 2.** Properties of the materials calculated on the basis of the nanoindentation data [11].

| Material | *H* | *E* | *R* |
|---|---|---|---|
| | GPa | GPa | % |
| Multilayer film Ti/α-C:H | 8.0 | 128 | 34 |
| Amorphous tape Zr-Cu-Ti-Ni | 11.5 | 117 | 42 |
| Silicon (100) | 11.8 | 174 | 62 |
| Thin film Ti-Si-N | 28.4 | 295 | 62 |

The comparison shows that the nanohardness of 12X18H10T+Ti coating in nitrogen atmosphere exceeds that of all the materials in Table 2, among which the last three materials are used as abrasive and hardening coatings. The nanohardness of Cr-Mn-Si-Cu-Fe-Al+Ti coating in nitrogen gas environment is almost 2 times higher than that of the pure titanium (*H* = 4.1 GPa) and close to the nanohardness of the multilayer film Ti/α-C:H.

Figure 3 shows the cellular structure of the coating. The same structure can also be observed for 12X18H10T+Ti coating in nitrogen atmosphere. A cellular substructure is often formed during

Репозиторий КарГУ

solidification as a result of the concentration supercooling [12]. If in formation of a cellular structure the zone of liquid melt enriched with impurities occurs at the crystallization front, the emergence of the impurity segregation at the cell boundaries can be attributed to the lateral impurity diffusion flux from the top of the growing projection. This model can be used to explain the observed cellular nanostructures with titanium nitride as a dopant. However, the cause of self-organization of the crystallizing melt on the substrate surface is to be found.

To address the issue of self-organization of structural units of the coating, consider the Bénard cell model. The Bénard cell phenomenon is the emergence of self-organization of convection cells in the form cylindrical shafts or regular hexagonal patterns in the layer of viscous fluid with a vertical temperature gradient [13]. Benard cells are one of the three standard examples of self-organization, along with the laser and the Belousov-Zhabotinsky reaction [14]. The temperature gradient is the governing parameter of self-organization.

More strictly (see, as an example, [13]) in the analysis of processes in the Bénard system, the governing parameter is the Rayleigh number:

$$\mathrm{Re} = gL^3bdT / \nu a,$$

where $g$ is gravitational acceleration, $L$ is the characteristic size, $b$ is the coefficient of volumetric expansion, d$T$ is the temperature gradient, $\nu$ is kinematic viscosity, and $a$ is the coefficient of thermal conductivity.

Since the kinematic viscosity $\nu \sim 1/\sigma$, $\sigma$ is surface tension, then the above expression for the Rayleigh number indicates that in this case (and presumably in the case of the Bénard process), surface tension is the governing parameter. Thereby, we return to the issues discussed above.

The above consideration on the formation of the plasma coating structure points out a more complicated situation than it might appear at first sight. Consider this issue at another angle, namely, using the model of dislocation cell structure (DCS). Inelastic deformation of crystals (and coatings) accompanied by the formation of the deformation relief on their surface, which reflects the process of deformation localization at meso-, micro- and nanoscale levels. Dislocation cell structure starts to form in a deformed crystal at the end of the second stage and at the beginning of the third stage of strain hardening of metals, and finishes at the end of the third stage (see [15] and references therein). In further deformation, a fragmented dislocation structure is formed (FDS) (at the fourth and fifth stages of strain hardening).

DCS is considered to be the process of self-organization of dislocations under multiple slip. For its occurrence, the specific criteria (as in the case of Bénard cells) binding together the coefficients of multiplication, immobilization, and dislocationannihilation are to be met.

In ion-plasma coating and coating cooling, stress states are formed in the latter [16]. These stress states can be the sources of dislocation propagation throughout the volume of the deposited coating. A sharp increase in microhardness of the formed film is the result of dislocation hardening the coating material. [17]. In [18], a sharp increase in microhardness was observed under ion-plasma deposition of high entropy alloys in nitrogen atmosphere.

**4. Conclusion**

From the results of the research into the formation of multiphase coatings we may draw the following conclusions:

- types of structures formed in ion-plasma deposition of coatings are not as diverse as, for example, in alloy crystallization. Basically, it is a globular structure and, rarely, unclosed dissipative and cellular structures;
- physical properties of the coatings can significantly vary depending on their composition of elements;
- since the value of the surface tension (surface energy) in most cases is an additive quantity, each element, being the part of the coating, contributes to the total surface energy;

Репозиторий КарГУ

- in case of simultaneous multiphase cathode sputtering, high entropy coatings are formed. They possess an ordered structure and improved mechanical properties.

Thus, the general pattern obtained is as follows: multi-phase (multi-element) cathodes should be used for superhard nanostructured coatings, preferably in simultaneous sputtering.

**5. Acknowledgements**

This work was financially supported by The Ministry of Education and Science of the Russian Federation in part of the science activity program.

**References:**

[1] Movchan B A, Demchishin A V 1969 Investigation of the structure and properties of nickel, titanium, tungsten, alumina, and zirconia thick vacuum condensates *Fizika metallov i metallovedenie* **4** 23.
[2] Thornton J A High rate thick film growth 1977 *Annual Review of Material Science* **7** 239.
[3] Barna P B, Adamik M 1977 *In Protective Coatings end Thin Films* Edited Pfleau Y, Barna P B. (Kluwer Academic, Dortrecht, The Netherlans) pp 279–297.
[4] Watanabe H., Sato Y., Nie C, Ando A, Ohtani S, Iwamoto N 2003 The mechenical properties and microstructure of Ti-Si-N nanocomposite films by ion plating *Surf. Coat. Technol*. **169–170** 452.
[5] Carvalho S, Ribeiro E, Rebouta L, Vaz F, Alves E, Schneider D, Cavaleiro A 2003 Effects of the morphology and structure on the elastic behavior of (Ti,Si,Al)N nanocomposites *Surf. Coat. Technol*. **174–175** 984.
[6] Flink A, Larsson T, Sjolen J, Karlsson L, Hultman L 2005 Influence of Si on the microstructure of arc evaporated (Ti,Si)N thin films; evidence for cubic solid solutions and their thermal stability *Surf. Coat. Technol*. **200** 1535.
[7] Li Z G, Mori M, Miyake S, Kumagai M, Saito H, Muramatsu Y 2005 Structure and properties of Ti-Si-N films prepared by ICP assisted magnetron sputtering *Surf. Coat. Technol.* **193** 345.
[8] Yurov V M, Laurinas V Ch, Guchenko S A, Zavatskaya O N 2014 Surface tension of hardening coatings *Uprochnyayushie tehnologii i pokrytiya* **1** 33.
[9] Jurov V M 2011 Superficial tension of pure metals *Eurasian Physical Technical Journal* **8** 10.
[10] Kidyarov B I 1979 *Kinetic of crystal formation from liquid phase* (Novosibirsk: Nauka) p 134.
[11] Golovin Yu I 2008 Nanoindentation and mechanical properties of solids in submicrovolumes, thin near-surface layers, and films: A Review *Physics of the Solid State* **50** 2205.
[12] Vayngard W 1967 *Introduction to the physics of metal crystallization* (Moscow: Mir) p 170.
[13] Gershuni G Z, Zhukhovnitsky E M 1972 *Convective stability of incompressible fluid* (Moscow: Nauka) p 232.
[14] Haken H 1991 *Information and self-organization: Macroscopic approach to complex systems* (Moscow: Mir) p 240.
[15] Malygin G A 2007 Simulation of the surface deformation relief of a plastically deformed crystal *Physics of the Solid State* **49** 1460.
[16] Barvinok V A 1990 *Control of the stress state and properties of plasma coatings* (Moscow: Mashinostroenie) p 384.
[17] Goryachev S E 1984 *Microscopic mechanisms of strain hardening* (Moscow: Moscow Engineering Physics Institute) p 61.
[18] Sobol' O V, Andreev A A, Gorban V F, Krapivka N A , Stolbovoi V A, Serdyuk I V, Fil'chikov V E 2012 Reproducibility of the single-phase structural state of the multielement high-entropy Ti-V-Zr-Nb-Hf system and related superhand nitrides formed by the vacuum-arc method *Technical Physics Letters* **38** 616.

Репозиторий КарГУ